0026-895X/98/050908-08$3.00/0

MOLECULAR PHARMACOLOGY, **53:**908–915 (1998).

A Comparison of Thermodynamic Parameters for Vinorelbine- and Vinflunine-Induced Tubulin Self-Association by Sedimentation Velocity

SHARON LOBERT, JEFFREY W. INGRAM, BRIDGET T. HILL, and JOHN J. CORREIA

School of Nursing (S.L.) and Department of Biochemistry, University of Mississippi Medical Center, Jackson, Mississippi 39216 (S.L., J.W.I., J.J.C.), and the Division de Cancerologie Experimentale, Centre de Recherche Pierre Fabre, 81106 Castres Cedex 06, France (B.T.H.)

Received November 11, 1997; Accepted February 2, 1998

This paper is available online at http://www.molpharm.org

ABSTRACT

We present a comparison of the energetics of spiral formation for two vinca alkaloids: a novel difluorinated vinorelbine derivative 20′,20′-difluoro-3′,4′-dihydrovinorelbine (F12158, or vinflunine) and the parent compound, vinorelbine. Vinca alkaloids are antineoplastic agents that halt cell division at metaphase by inhibiting microtubule assembly and inducing tubulin self-association into spiral aggregates. The overall affinities for tubulin of vincristine, vinblastine, and vinorelbine seem to correlate with their clinical doses, where vincristine with the highest overall affinity is used at the lowest doses. Doses of chemotherapeutic agents, however, also are determined by toxicities. In the physicochemical study described here, we used sedimentation velocity to compare vinorelbine- and vinflunine-induced self-association of porcine brain tubulin in the presence of 50 μM GDP or 50 μM GTP. Vinflunine demonstrates 3–16-fold lower overall affinity for tubulin and induces smaller polymers compared with vinorelbine. Sedimentation velocity provides the only direct evidence to date that vinflunine is a tubulin-binding drug. Stopped-flow light scattering demonstrates the shortest relaxation times for polymer redistribution for vinflunine consistent with induction of the shortest spirals. Data collected at 5°, 15°, 25°, and 37° show increasing $\bar{s}_{20,w}$ values with increasing temperature and are consistent with an entropically driven process. These data are entirely consistent with our hypothesis that vinflunine is likely to result in reduced clinical neurotoxicity relative to vinorelbine, vinblastine, and vincristine.

The antineoplastic properties of vinca alkaloids arise from their interaction with tubulin, the major component of microtubules in mitotic spindles. These drugs diminish microtubule dynamics and assembly, resulting in the arrest of cell division at metaphase. At substoichiometric levels, *in vitro*, vinca alkaloids stabilize microtubules, possibly by binding to microtubule ends and inhibiting hydrolysis of GTP (Jordan and Wilson, 1990; Jordan *et al*., 1991; Toso *et al*., 1993). At higher concentrations, microtubules depolymerize, and in the presence of MAPs or at high magnesium concentrations (>2.5 mM), vinca alkaloids induce large paracrystals made up of spiral helices of one or two protofilaments (Fujiwara and Tilney, 1975; Amos *et al*., 1984; Timasheff, 1986a, 1986b; Himes, 1991; Na and Nogales *et al*., 1995).

Three vinca alkaloids that are currently important in anticancer chemotherapy protocols, vincristine, vinblastine, and vinorelbine, are used for treating a spectrum of solid and hematological tumors (Lobert and Correia, 1992; Johnson *et al*., 1996). As antimitotic drugs, their affinity for tubulin has an impact on drug efficacy and toxicity. The order of overall affinity for tubulin is vincristine > vinblastine > vinorelbine (Lobert *et al*., 1996). This relative drug affinity for tubulin may be related to the clinical doses used; generally, vincristine is administered at 2 mg/m^2 and vinorelbine at 30 mg/m^2 (Lobert and Correia, 1992; Chabner *et al*., 1996). However, clinical doses also are based on dose-limiting side effects. The clinical toxicity of vincristine is mostly neurological, with predictable cumulative effects, whereas vinorelbine is the least neurotoxic vinca alkaloid (Chabner *et al*., 1996). Our hypothesis is that the overall drug affinity for tubulin contributes to the severity of the neuropathies observed clinically. In fact, this is currently the basis for clinical trials with vinorelbine.

Vinca alkaloid binding is linked to tubulin self-association, and the binding affinities can be determined by sedimentation velocity. These data are best fit by an isodesmic ligand-mediated or ligand-mediated plus ligand-facilitated model (Na and Timasheff, 1980, 1986a). The major difference between the drugs is in K_2, the affinity of liganded heterodimers for spirals, and in K_3, the binding of drug to polymers. All three drugs show an increase in maximum $\bar{s}_{20,w}$

This work supported by National Institutes of Health Grant NR00056 (S.L.) and by Institut de Recherche Pierre Fabre.

ABBREVIATIONS: EGTA, ethylene glycol bis(β-aminoethyl ether)-*N*,*N*,*N*′,*N*′-tetraacetic acid; GXP, GTP or GDP; MAP, microtubule associated protein; PC-tubulin, MAP-free phosphocellulose purified tubulin; PIPES, piperazine-*N*,*N*′-bis(2-ethanesulfonic acid).

values with increasing temperature, consistent with an entropically driven process. The relative magnitudes of K_2 were independently confirmed by stopped-flow light scattering, in which relaxation times, τ, are longest for vincristine polymers and shortest for vinorelbine polymers (Lobert *et al*., 1996). Furthermore, there is a decrease in τ with increasing tubulin concentration, suggesting annealing of oligomers in addition to association of liganded-heterodimers (Thusius *et al*., 1975; Nogales *et al*., 1995; Lobert *et al*., 1996).

In the current work, we compared the energetics of tubulin spiral formation in the presence of a novel difluorinated derivative of vinorelbine, vinflunine (Fahy *et al*., 1997), with the parent compound using sedimentation velocity. We found that vinflunine induces significantly smaller spirals than vinorelbine. The difference between the two drugs is primarily in K_2, the affinity of liganded-heterodimers for spirals, and in K_3, the affinity of drug for polymers. Van't Hoff analysis of data collected at 5°, 15°, and 25° shows more positive $\Delta H°$ and $\Delta S°$ for vinflunine compared with vinorelbine, consistent with an entropically driven process. The increased $\Delta H°$ corresponds to a less negative (less favorable) $\Delta G°$ for vinflunine. Stopped-flow light scattering was used to investigate the mechanism of drug-induced spiral formation. Vinflunine demonstrates shorter relaxation times compared with vinorelbine, and the data are consistent with spiral formation occurring by the addition of liganded heterodimers and the annealing of oligomers. These data together suggest that vinflunine may demonstrate reduced neurotoxicity relative to the other three vinca alkaloids. Our sedimentation velocity studies are the only direct evidence that vinflunine is a tubulin-binding drug and therefore contribute to understanding of its potential as a clinically useful antimitotic agent.

Experimental Procedures

Reagents. Deionized (Nanopure) water was used in all experiments. $MgSO_4$, EGTA, GDP (type I), GTP (type II-S), and PIPES were purchased from Sigma Chemical (St. Louis, MO). Sephadex G-50 was from Pharmacia (Piscataway, NJ).

Tubulin purification. Porcine brain tubulin (PC-tubulin) free of MAPs was obtained by two cycles of warm/cold polymerization/depolymerization followed by phosphocellulose chromatography to separate tubulin from MAPs (Williams and Lee, 1982; Correia *et al*., 1987). Protein concentrations were determined spectrophotometrically (ϵ_{278} = 1.2 liter/g·cm) (Detrich and Williams, 1978).

Sedimentation velocity experiments. Vinorelbine- or vinflunine-induced tubulin spiral formation was studied in the presence of GDP or GTP by sedimentation velocity. Vinorelbine, as the tartrate, was obtained from Pierre Fabre Medicaments (Gaillac, France), and vinflunine sulfate was kindly provided by Dr. J. Fahy (Center de Recherche Pierre Fabre, Castres, France). Tubulin samples (2 μM) were equilibrated in 10 mM PIPES, pH 6.9, 2 mM EGTA, 1 mM $MgSO_4$, and 50 μM GXP using spun columns (Lobert *et al*., 1995). The free drug concentration (0.5–70 μM) was obtained from the known drug concentration in the equilibration buffer. For vinflunine, the extinction coefficients are $\epsilon_{214,\ water}$ = 61,650 M^{-1} cm^{-1} and $\epsilon_{268,\ water}$ = 18,650 M^{-1} cm^{-1}, and for vinorelbine, they are $\epsilon_{215,\ water}$ = 57,800 M^{-1} cm^{-1} and $\epsilon_{268,\ water}$ = 17,150 M^{-1} cm^{-1} (Institut de Recherche Pierre Fabre). In previous work (Lobert *et al*., 1996), stock clinical solutions were purchased from Glaxo-Wellcome (Research Triangle Park, NC). The stated concentration was interpreted as 10 mg/ml vinorelbine ditartrate, although as noted recently, the solutions were actually 10 mg/ml vinorelbine. Thus, for comparison with the data collected here, the vinorelbine concentrations from our previous work (Lobert *et al*., 1996) were corrected by a factor of nearly 1.4. After equilibration, the protein was brought to the desired final concentration by dilution with the equilibration buffer. Sedimentation studies were done in a Beckman Instruments (Palo Alto, CA) Optima XLA analytical ultracentrifuge equipped with absorbance optics and an An60 Ti rotor. Samples were spun at 5°, 15°, 25°, or 37° at appropriate speeds, and temperature was calibrated according to the method of Liu and Stafford (1995). Velocity data were collected at 278 nm and at a spacing of 0.002 cm with one average in a continuous scan mode. Data were analyzed using software (DCDT) provided by Dr. Walter Stafford (Boston Biomedical Research Institute, Boston, MA) to generate a distribution of sedimentation coefficients, $g(s)$ (Lobert *et al*., 1995).

Curve fitting of sedimentation velocity data. The distributions of sedimentation coefficients, $g(s)$, were converted to weight average $\bar{s}_{20,w}$ values by integration of the curves ($\int s * g(s)ds/\int g(s)ds$) using Origin 3.5 (Microcal Software, Northampton, MA) and correction for temperature and buffer components. The data were plotted as weight average $\bar{s}_{20,w}$ values versus free drug. Total protein concentration for each sample was determined from $\int g(s)ds$. Sedimentation data were fit using the isodesmic ligand-mediated or the isodesmic ligand-mediated plus ligand-facilitated model (also referred to as the combined model) (Lobert *et al*., 1995). In these models, K_1 is the affinity of drug for tubulin heterodimers, K_2 is the affinity of liganded heterodimers for spiral polymers, K_3 is the affinity of drug for polymers, and K_4 is the association constant for unliganded-tubulin heterodimers. Binding constants and error estimates were obtained by fitting with the nonlinear least-squares program Fitall (MTR Software, Toronto, Canada), modified to include the appropriate fitting functions. We find that in the combined model fit, it is necessary to constrain K_4, the association constant for unliganded tubulin heterodimers, to 1×10^4 M^{-1} to compare the binding affinities because only three binding constants are independent in this scheme. As with any linear and nonlinear least-squares procedures, the fitted parameters exhibit a certain degree of cross-correlation, and the overall product, K_1K_2, is probably better determined than the individual parameters, K_1 and K_2. However, the results demonstrate that K_1 is nearly a constant for both drugs, $9.75 \pm 2.62 \times 10^4$ M^{-1} (average for the ligand-mediated fits at 5°, 15°, and 25°), and that the major difference between drugs and the major effect of GDP is in the value of K_2. This is compelling evidence that we are correctly determining reliable parameters.

Stopped-flow light-scattering experiments. Stopped-flow rapid mixing experiments (manual stopped-flow apparatus; Hi-Tech, Wiltshire, England) were carried out as described previously (Lobert *et al*., 1996). Briefly, PC-tubulin (0.6–4 μM) was equilibrated, using spun columns, into 10 mM PIPES, pH 6.9, 2 mM EGTA, 1 mM $MgSO_4$, 50 μM GTP, and 70 μM vinorelbine or vinflunine. The final drug and tubulin concentrations were 35 and 0.3–2 μM, respectively. Samples were degassed for 1 hr at room temperature. Stopped-flow rapid-mixing experiments at 25° were initiated by diluting tubulin samples 1:1 with the same buffer without drug. Relaxation was monitored using an SLM Aminco Bowman Series 2 Luminescence Spectrometer (Rochester, NY) at 350 nm (90-degree scattering) over 10 min. Relaxation times, τ, were determined using the following equation: $x = a_0\exp(-t/\tau)$, where a_0 is the change in amplitude associated with τ over time, t (sec). We used χ^2 determinations to select the best fits of the data using Origin 3.5.

Results

Vinorelbine- and vinflunine-induced tubulin spiral formation. The association of 2 μM PC-tubulin (10 mM PIPES, pH 6.9, 1 mM $MgSO_4$, 2 mM EGTA, 50 μM GXP) in the presence of vinorelbine or vinflunine (0.5–70 μM) was studied with the use of sedimentation velocity at 5°, 15°, 25°, and 37°.

Fig. 1 shows weight average sedimentation coefficients, $\bar{s}_{20,w}$, plotted versus drug concentrations for both drugs at each temperature. We found that increasing the temperature resulted in larger $\bar{s}_{20,w}$ values for vinorelbine and vinflunine, although the maximum s values in the presence of vinflunine are considerably smaller than those for vinorelbine. For example, at 37° in the presence of GDP (Fig. 1a), the maximum $\bar{s}_{20,w}$ values for vinorelbine are ~18 S, whereas for vinflunine, the maximum values are near 11 S. Data were fit with the ligand-mediated model or ligand-mediated plus ligand-facilitated (combined) model to obtain equilibrium constants (Tables 1 and 2). Fits with either the ligand-mediated model or combined model were indistinguishable in terms of the standard deviation of the fits. At 5°, 15°, and 25°, vinorelbine interacts with tubulin with 3–16-fold higher overall affinity, K_1K_2, than vinflunine, depending on the model used to determine the binding parameters (Tables 1 and 2). Thus, the modifications involving the C20′ difluorination (IUPAC numbering system is used throughout) and the lack of the 3′,4′ double bond in vinflunine may result in this decrease in its overall affinity for tubulin.

The fitted parameters determined at 37° do not show this difference between vinorelbine and vinflunine. We observed in the 37° data a prominent 20 S shoulder in the $g(s)$ plots at low drug concentration. To investigate the significance of these larger aggregates, we carried out sedimentation velocity studies with 2 μM tubulin in the absence of drug over a range of temperatures of 25–37° (data not shown). We found that at temperatures of ≥30°, the 20 S shoulder becomes significant, indicating the formation of higher order aggregates, probably due to tubulin denaturation. At low drug concentrations, there is a small but significant portion of the unliganded tubulin at 37° forming larger aggregates that sediment faster than the liganded tubulin spirals. Because of the aggregation of unliganded tubulin, we used only data from 3–70 μM in fitting the 37° data, rather than from 0.5–70 μM (Tables 1 and 2). Even with this editing, the ligand-mediated models may not describe the data collected at 37°, and the binding parameters may be unreliable. A more detailed study of high temperature tubulin denaturation will be presented elsewhere (Vulevic B, Lobert S, and Correia JJ, manuscript in preparation).

The K_2^{app} is the drug-dependent indefinite self-association constant for tubulin spiral formation (Na and Timasheff, 1985). Because self-association is linked to drug binding, it is a measure of the extent of overall drug binding. Fig. 2 shows plots of K_2^{app} versus free drug concentrations for the data collected in the presence of GDP (Fig. 2a) or GTP (Fig. 2b) and fit with the ligand-mediated model. The K_2^{app} was calculated from individual binding affinities, K_1 and K_2, as described in the legend. It is clear that significantly more spiral formation occurs with vinorelbine than with vinflunine at all temperatures studied. According to the Wyman (1964) linkage theory, this means that more vinorelbine binds to tubulin than vinflunine under all comparable conditions.

We do not find a significant difference in K_1, drug binding to tubulin heterodimers, for vinorelbine and vinflunine (Tables 1 and 2). The mean K_1 values found in these studies at 5°, 15°, and 25° for vinorelbine and vinflunine (both nucleotides and both models) are $9.5 \pm 3.0 \times 10^4$ M^{-1} and $6.5 \pm 2.7 \times 10^4$ M^{-1}, respectively. Note that our previous value for vinorelbine under similar conditions, 5° and 25°, was $1.1 \pm 0.3 \times 10^5$ M^{-1} (Lobert *et al.*, 1996). The low degree of association with these drugs potentially makes parameter estimation difficult. To verify the reliability of K_1 values, we carried out titrations of 4 μM tubulin with vinorelbine and vinflunine in the presence of GTP at 25° (Table 1). At this higher protein concentration, the extent of association is enhanced, and in

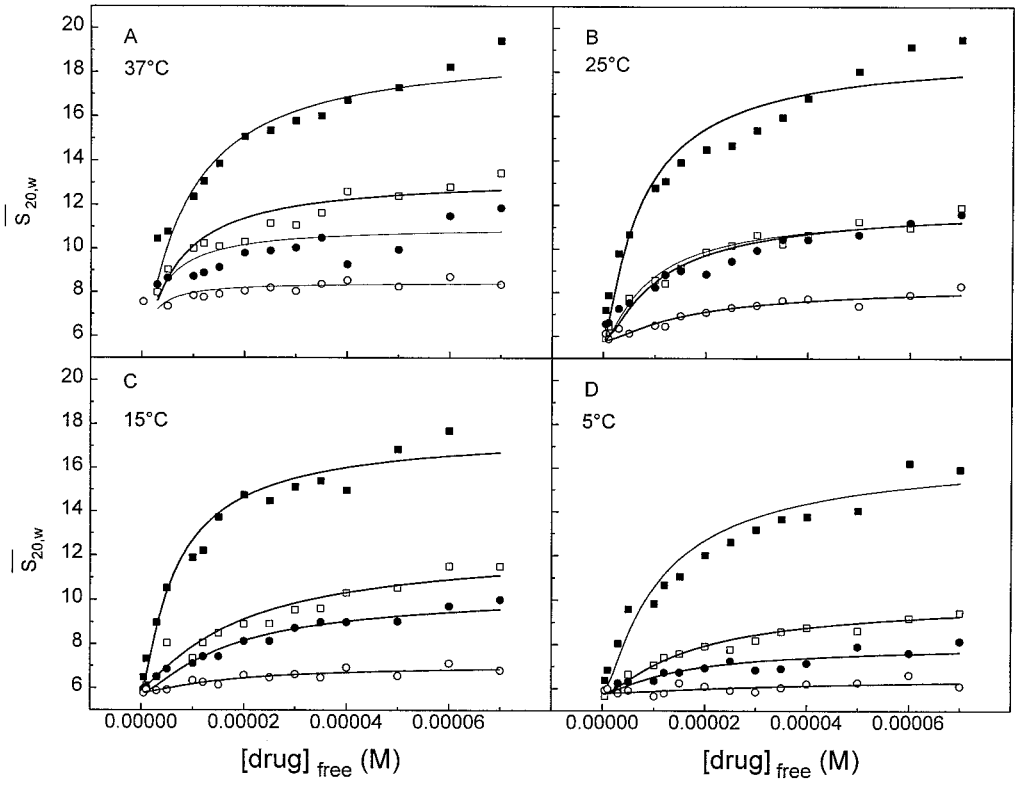

Fig. 1. Plots of $\bar{s}_{20,w}$ values versus free concentrations of vinorelbine (■, □) or vinflunine (●, ○) at 37° (A), 25° (B), 15° (C), or 5° (D). Tubulin in all experiments was 2 μM in the presence of 50 μM GTP (*open symbols*) or GDP (*closed symbols*). *Solid lines*, fits using the ligand-mediated model. The equilibrium constants obtained from these fits are given in Tables 1 and 2.

principle, parameter estimation should be improved. We obtained nearly identical K_1 values compared with the 2 μM tubulin data, 1.1 ± 0.3 × 10^5 M^{-1} and 7.2 ± 3.4 × 10^4 M^{-1}, averaged over both models for vinorelbine and vinflunine (Table 1). For the 2 μM tubulin data at 25°, the K_1 values were 1.2 ± 0.2 × 10^5 M^{-1} and 6.9 ± 2.8 × 10^4 M^{-1}. Thus, within the error of these measurements, there is no difference in K_1 values for these two drugs.

The difference between vinorelbine- and vinflunine-induced spiral formation at 5°, 15°, 25°, and 37° is primarily in K_2, liganded heterodimers binding to spirals, when data are fit with either model (Tables 1 and 2). For vinorelbine data fit with the ligand-mediated model, K_2 is 4–14-fold larger than that for vinflunine. This amounts to 0.82–1.56 kcal/mol enhancement for vinorelbine compared with vinflunine. For the combined model, the K_2 enhancement by vinorelbine is smaller, only 2–7-fold (0.41–1.15 kcal/mol), whereas the enhancement in K_3, drug binding to polymers, is 3–16-fold (0.65–1.64 kcal/mol). Thus, spiral formation and drug binding to spirals are significantly reduced in the presence of vinflunine compared with vinorelbine.

GDP enhancement of vinorelbine- and vinflunine-induced tubulin spiral formation. GDP enhances vinorelbine- and vinflunine-induced tubulin self-association (Fig. 1 and Table 3). The mean GDP enhancement in K_1K_2 for the data collected at 5°, 15°, and 25° is equal to 0.84 ± 0.20 kcal/mol for data fit with both models (Table 3). This agrees well with our previous report of a mean GDP enhancement of 0.90 ± 0.17 kcal/mol for vinblastine, vincristine, and vinorelbine (Lobert *et al.*, 1996). When data are fit with the ligand-

TABLE 1
Equilibrium constants for the interaction of vinca alkaloids with tubulin

Drug	Temperature	GXP	K_1	K_2	K_3	K_1K_2	Standard deviation
				M^{-1}		M^{-2}	
2 μM tubulin							
Vinorelbine	5°	GTP	7.4 × 10^4 ± 1.2	6.7 × 10^5 ± 0.7		5.0 × 10^{10}	0.2[a]
			4.7 × 10^4 ± 0.7	9.1 × 10^4 ± 3.1	4.3 × 10^5 ± 0.7	4.3 × 10^9	0.2[b]
Vinflunine			4.4 × 10^4 ± 4.3[c]	7.3 × 10^4 ± 5.0		3.2 × 10^9	0.2[a]
			1.3 × 10^4 ± 3.1	4.9 × 10^4 ± 16.0	6.4 × 10^4 ± 12.0	6.4 × 10^8	0.3[b]
Vinorelbine	15°		7.7 × 10^4 ± 1.8	1.3 × 10^6 ± 0.2		1.0 × 10^{11}	0.5[a]
			5.4 × 10^4 ± 0.5	1.2 × 10^5 ± 0.2	6.5 × 10^5 ± 0.5	6.5 × 10^9	0.4[b]
Vinflunine			9.7 × 10^4 ± 3.0	1.3 × 10^5 ± 0.2		1.3 × 10^{10}	0.1[a]
			3.9 × 10^4 ± 0.5	4.2 × 10^4 ± 1.0	1.6 × 10^5 ± 0.2	1.6 × 10^9	0.2[b]
Vinorelbine	25°		1.3 × 10^5 ± 0.2	1.1 × 10^6 ± 0.8		1.4 × 10^{11}	0.3[a]
			1.0 × 10^5 ± 0.05	1.1 × 10^5 ± 0.1	1.1 × 10^6 ± 0.4	1.1 × 10^{10}	0.3[b]
Vinflunine			8.8 × 10^4 ± 2.0	3.0 × 10^5 ± 0.4		2.6 × 10^{10}	0.2[a]
			4.9 × 10^4 ± 0.1	6.0 × 10^4 ± 0.3	2.9 × 10^5 ± 0.1	2.9 × 10^9	0.2[b]
Vinorelbine	37°		1.6 × 10^5 ± 0.3	1.6 × 10^6 ± 0.1		2.6 × 10^{11}	0.5[a]
			1.3 × 10^5 ± 0.03	1.3 × 10^5 ± 0.06	1.7 × 10^6 ± 0.03	1.7 × 10^{10}	0.5[b]
Vinflunine			6.4 × 10^5 ± 1.7	3.2 × 10^5 ± 0.2		2.1 × 10^{11}	0.2[a]
			4.6 × 10^5 ± 0.7	5.6 × 10^4 ± 2.2	2.6 × 10^6 ± 0.4	2.6 × 10^{10}	0.3[b]
4 μM tubulin							
Vinorelbine	25°		1.3 × 10^5 ± 0.2	1.1 × 10^6 ± 0.07		1.4 × 10^{11}	0.4[a]
			9.3 × 10^4 ± 0.4	1.1 × 10^5 ± 0.1	1.0 × 10^6 ± 0.04	1.0 × 10^{10}	0.3[b]
Vinflunine			9.6 × 10^4 ± 1.9	2.7 × 10^5 ± 0.3		2.6 × 10^{10}	0.3[a]
			4.8 × 10^4 ± 0.1	5.7 × 10^4 ± 0.2	2.7 × 10^5 ± 0.04	2.7 × 10^9	0.2[b]

[a] Data were fit with the ligand-mediated model.
[b] Data were fit with the combined ligand-mediated plus-facilitated model, and K_4 was constrained to be 1 × 10^4 M^{-1}.
[c] Note that the error for these parameters is larger than those found in other data sets. This is most likely due to the low level of spiral formation with this drug, especially at low temperature, and therefore very shallow data curves are fit with the two models. We find that the standard deviations of the fits are equivalent to other data sets and therefore the estimates of binding affinities are useful for comparing data collected under other conditions.

TABLE 2
Equilibrium constants for the interaction of vinca alkaloids with tubulin

Drug	Temperature	GXP	K_1	K_2	K_3	K_1K_2	Standard deviation
				M^{-1}		M^{-2}	
2 μM tubulin							
Vinorelbine	5°	GDP	8.6 × 10^4 ± 1.6	3.8 × 10^6 ± 0.4		3.3 × 10^{11}	0.7[a]
			7.0 × 10^4 ± 0.5	2.0 × 10^5 ± 0.3	1.4 × 10^6 ± 0.09	1.4 × 10^{10}	0.6[b]
Vinflunine			9.9 × 10^4 ± 3.1	2.8 × 10^5 ± 0.4		2.8 × 10^{10}	0.2[a]
			4.9 × 10^4 ± 0.6	5.8 × 10^4 ± 1.2	2.8 × 10^5 ± 0.3	2.8 × 10^9	0.2[b]
Vinorelbine	15°		1.4 × 10^5 ± 0.2	4.8 × 10^6 ± 0.3		6.7 × 10^{11}	0.5[a]
			1.2 × 10^5 ± 0.06	2.2 × 10^5 ± 0.2	2.6 × 10^6 ± 0.1	2.6 × 10^{10}	0.5[b]
Vinflunine			7.4 × 10^4 ± 1.5	8.4 × 10^5 ± 1.0		6.2 × 10^{10}	0.3[a]
			4.8 × 10^4 ± 0.4	9.8 × 10^4 ± 1.4	4.7 × 10^5 ± 0.3	4.7 × 10^9	0.3[b]
Vinorelbine	25°		1.3 × 10^5 ± 0.3	5.1 × 10^6 ± 0.6		6.6 × 10^{11}	1.0[a]
			1.1 × 10^5 ± 0.1	2.3 × 10^5 ± 0.4	2.5 × 10^6 ± 0.2	2.5 × 10^{10}	1.0[b]
Vinflunine			1.0 × 10^5 ± 0.3	1.2 × 10^6 ± 0.2		1.2 × 10^{11}	0.5[a]
			7.5 × 10^4 ± 0.2	1.1 × 10^5 ± 0.1	8.5 × 10^5 ± 0.2	8.5 × 10^9	0.5[b]
Vinorelbine	37°		1.1 × 10^5 ± 0.2	6.0 × 10^6 ± 0.6		6.6 × 10^{11}	0.8[a]
			9.2 × 10^4 ± 0.6	2.5 × 10^5 ± 0.4	2.3 × 10^6 ± 0.1	2.3 × 10^{10}	0.7[b]
Vinflunine			3.1 × 10^5 ± 0.9	9.3 × 10^5 ± 0.9		2.9 × 10^{11}	0.6[a]
			2.3 × 10^5 ± 0.5	9.4 × 10^4 ± 5.9	2.2 × 10^6 ± 0.6	2.2 × 10^{10}	0.6[b]

[a] Data were fit with the ligand-mediated model.
[b] Data were fit with the combined ligand-mediated plus-facilitated model, and K_4 was constrained to be 1 × 10^4 M^{-1}.

mediated model, the effect of GDP occurs primarily on K_2, the affinity for association of liganded heterodimers, rather than on K_1, the affinity for drug binding to the heterodimer. For the combined model, the GDP enhancement occurs primarily in K_2 and K_3. This is consistent with our expectations of Wyman linkage, where drug binding enhances self-association and self-association enhances drug binding (Lobert *et al.*, 1995).

Comparison of vinorelbine and vinflunine thermodynamic parameters. Table 4 gives the thermodynamic parameters obtained from Van't Hoff analysis of the data collected at 5°, 15°, and 25°. As discussed, the equilibrium constants determined from fits of the data at 37° are not reliable and thus were not used in this analysis. The overall affinity, K_1K_2, from ligand-mediated fits was used to calculate ΔG. Similar results were obtained from combined model fits (data not shown). Plots of $\ln K_1K_2$ versus 1/T were used to determine ΔH (data not shown). The free energy, ΔG°, at 25°, for vinflunine binding in the presence of GTP was less negative than that for vinorelbine binding: −14.2 and −15.2 kcal/mol, respectively. In the presence of GDP, the values were −15.1 and −16.1, respectively. Thus, the smaller K_2 and K_1K_2 values for vinflunine-induced tubulin self-association are reflected in the less negative ΔG. The ΔH° and ΔS° values are consistent with an entropically driven polymerization process, although the absolute values are model dependent (Table 4). The unfavorable ΔH° in general is compensated by a positive ΔS°, regardless of the model used to fit the data. We showed previously that ΔH° is larger for drugs with smaller K_1K_2 values (Lobert *et al.*, 1996). Likewise in this case, ΔH° is larger for vinflunine compared with vinorelbine.

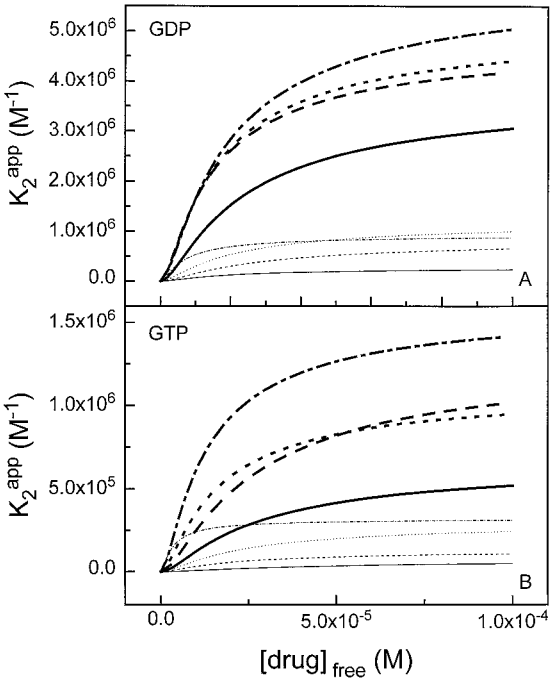

Fig. 2. Plots of $K_{2^{app}}$ versus free drug concentrations. The $K_{2^{app}}$ was calculated using equilibrium constants from ligand-mediated fits of the data $\{K_{2^{app}} = K_2/(1 + 1/K_1[\text{drug}])^2\}$. *Bold lines*, vinorelbine data. *Light lines*, vinflunine data. —, 5°; – –, 15°; - - -, 25°; – - – -, 37°. Data were collected in the presence of GDP (A) or GTP (B). The data fit with the combined model demonstrates the same difference for vinorelbine and vinflunine overall drug binding (data not shown).

Stopped-flow light-scattering drug dilution. To investigate the kinetics of drug-induced tubulin association, we used rapid-mixing stopped-flow light scattering (Fig. 3). Data were best fit with single exponentials to obtain the relaxation times given in Table 5. In this table, A1 represents the change in the light-scattering signal, and τ is the relaxation time in seconds. It can be seen that the relaxation times for vinflunine are slightly shorter than those for vinorelbine (range, 2.14–20.90 versus 10.68–25.25 sec, respectively). This is consistent with a model that involves a cascade of dissociation events from larger to smaller polymers on dilution. The larger polymers for vinorelbine versus vinflunine (Fig. 1) are consistent with these longer average relaxation events for vinorelbine. Furthermore, the relaxation time decreases with increasing tubulin concentration (Table 5). This has been observed previously in the relaxation data for vin-

TABLE 3
ΔΔG GDP enhancement

	Ligand-mediated fits		
	K_1	K_2	K_1K_2
			kcal/mol[a]
5°			
Vinorelbine	0.083	0.959	1.042
Vinflunine	0.448	0.742	1.198
15°			
Vinorelbine	0.342	0.747	1.088
Vinflunine	−0.154	1.067	0.894
25°			
Vinorelbine	0	0.908	0.918
Vinflunine	0.075	0.820	0.906
Mean			1.008 ± 0.123
37°			
Vinorelbine	−0.231	0.814	0.573
Vinflunine	−0.447	0.657	0.198

	Combined model fits			
	K_1	K_2	K_3	K_1K_2
			kcal/mol[a]	
5°				
Vinorelbine	0.220	0.435	0.655	0.652
Vinflunine	0.732	0.093	0.833	0.833
15°				
Vinorelbine	0.457	0.347	0.793	0.793
Vinflunine	0.119	0.485	0.617	0.617
25°				
Vinorelbine	0.056	0.437	0.486	0.486
Vinflunine	0.252	0.359	0.637	0.637
Mean[b]				670 ± 0.126
37°				
Vinorelbine	−0.213	0.403	0.186	0.186
Vinflunine	−0.427	0.319	−0.102	−0.102

[a] $\Delta\Delta G = \Delta G_{gdp} - \Delta g_{gtp}$
[b] For both models, the mean K_1K_2 enhancement 5°, 15°, and 25° = 0.839 ± 0.203.

TABLE 4
Thermodynamic parameters for tubulin-vinca alkaloid interaction at 25°

		Ligand-mediated			
		K_1K_2	ΔG°	ΔS°	ΔH°
		M^{-2}	*kcal/mol*	*cal/mol−°K*	*kcal/mol*
Vinorelbine					
GTP		1.4×10^{11}	−15.2	76	7.4[a]
GDP		6.6×10^{11}	−16.1	69	4.4[a]
Vinflunine					
GTP		2.6×10^{10}	−14.2	98	15.1[a]
GDP		1.2×10^{11}	−15.1	87	10.9[a]

[a] Data from three temperatures only (5°, 15°, and 25°).

blastine (Lobert *et al*., 1996) and in the synchrotron data of Nogales *et al*. (1995). It suggests that in addition to liganded heterodimers adding to or dissociating from polymers, oligomers can self-associate or dissociate in a mechanism consistent with annealing of spiral polymers.

To obtain the on rate, k_a, and the off rate, k_d, for vinorelbine and vinflunine, the squares of the reciprocals of the relaxation times ($1/\tau^2$) were plotted against the final tubulin concentrations (Table 6). Vinorelbine has a smaller off rate, k_d, than vinflunine: 0.043 and 0.185 sec^{-1}, respectively. However, the binding affinities, determined from the ratio k_a/k_d, are very similar (probably due to larger error in the light-scattering method): 5.6×10^5 M^{-1} and 5.4×10^5 M^{-1} for vinorelbine and vinflunine, respectively. Note that the K_2 values determined from sedimentation velocity data at 25°, fit with the ligand-mediated model, are reasonably consistent with this result: 1.1×10^6 M^{-1} and 3.0×10^5 M^{-1} for vinorelbine and vinflunine, respectively. Thus, we conclude that the mechanism of spiral formation for these two drugs is identical, meaning that spiral formation occurs by addition of heterodimers and oligomers.

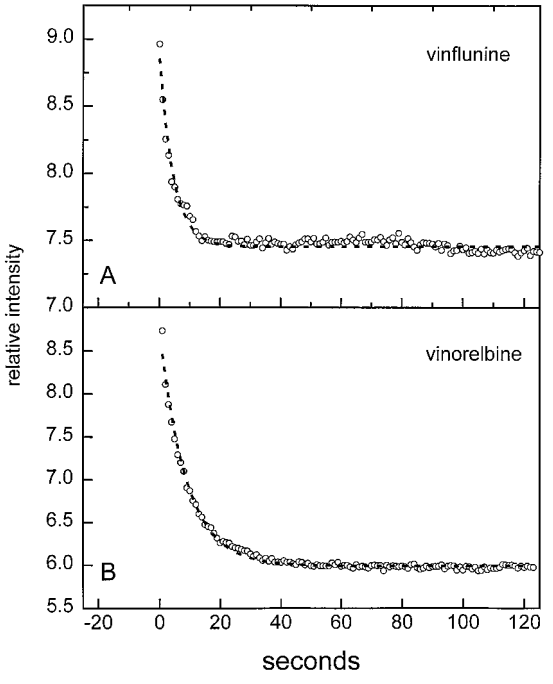

Fig. 3. Stopped-flow light-scattering experiments with vinflunine (A) and vinorelbine (B). The relative intensity is plotted versus time. The drug concentrations in this experiment were initially 70 μM, and the tubulin concentrations were initially 4 μM. The sample was diluted 1:1 with the appropriate buffer at the onset, and light scattering was monitored over 2 min at 1-sec intervals. *Dashed line*, single exponential fit of the data.

TABLE 5
Stopped-flow light scattering

Drug	[Tubulin] (initial)	A1[a]	τ
	μM		*sec*
Vinflunine	1.2	0.657 ± 0.085	20.90 ± 16.54
	1.4	0.412 ± 0.094	7.82 ± 4.40
	1.8	0.964 ± 0.184	2.65 ± 1.43
	2.8	1.399 ± 0.186	2.14 ± 0.97
	4.0	1.080 ± 0.233	2.71 ± 0.80
Vinorelbine	0.6	0.150 ± 0.018	25.25 ± 20.88
	1.0	0.378 ± 0.013	15.71 ± 4.12
	2.0	1.738 ± 0.216	11.00 ± 2.02
	4.0	2.676 ± 0.189	10.68 ± 3.21

[a] A1 is the change in light scattering signal, and τ is the relaxation time.
Drug dilution from 70 to 35 μM, 10 mM PIPES, pH 6.9, 2 mM EGTA, 1 mM $MgSO_4$, 50 μM GTP.

Discussion

Mechanism of vinca alkaloid-induced tubulin association. Stopped-flow light-scattering data demonstrated that vinorelbine, vinblastine, and vincristine-induced tubulin self-association occurs by a similar mechanism for all three drugs (Lobert *et al*., 1996). The relaxation data can be analyzed according to the theory developed by Thusius *et al*. (1975). They showed for glutamate dehydrogenase that relaxation times decrease with increasing protein concentration, indicating that self-association occurs by both association of single protein subunits to the ends of polymers and by association of oligomers. We propose that for all four vinca alkaloids investigated, vinorelbine, vinblastine, vincristine, and vinflunine, oligomer annealing can occur, in addition to liganded heterodimers adding to the ends of spirals. This is consistent with our proposed mechanism of microtubule inhibition in which spirals anneal to the ends of microtubules and suppress dynamics (Lobert *et al*., 1995, 1996, 1997). Within error, the binding affinity, K_{app}, values for vinorelbine and vinflunine determined by light-scattering kinetics are reasonably consistent with our sedimentation velocity data. Note that if light-scattering data collected here for vinorelbine are combined with previous light-scattering data collected for vinorelbine (Lobert *et al*., 1996), the estimated K_{app} is 9.4×10^5 M^{-1} rather than 5.6×10^5 M^{-1} as reported here in Table 6. These combined data give a value closer to the K_2 value estimated on the basis of sedimentation velocity at 25° (Table 1; $K_2 = 1.1 \pm 0.8 \times 10^6$ M^{-1}). These K_{app} values correspond to a $\Delta\Delta G°$, $\Delta G_{vinorelbine} - \Delta G_{vinflunine}$, of 0.33 kcal/mol. In other words, with light scattering measurements, spiral formation induced by vinorelbine is favored by 0.33 kcal/mol relative to vinflunine.

These kinetic data contribute to understanding the results of iodoacetamide alkylating experiments in the presence of vinca alkaloids (Kruczynski *et al*., 1998a). Over a 2-hr period, vincristine and vinblastine continue to inhibit alkylation of sulfhydryls, whereas in the presence of vinorelbine or vinflunine, alkylation is not inhibited. If tubulin in spirals is a poor substrate for alkylation, then the overall affinity for spiral formation should be a measure of inhibition of alkylation. Furthermore, smaller spirals will exchange tubulin heterodimers more readily. Relaxation times for vinorelbine-induced spirals are 2–3-fold shorter than those for vinblastine-induced spirals (Lobert *et al*., 1996). Relaxation times for vincristine-induced spirals are several-fold longer than those for vinblastine-induced spirals. We report

TABLE 6
Light scattering data

Drug	GXP	k_a	k_d	K_{app}
		$M^{-1}sec^{-1}$	sec^{-1}	M^{-1}
Vinorelbine	GTP	2.4×10^4	0.043	5.6×10^5
Vinflunine	GTP	1.0×10^5	0.185	5.4×10^5

Relaxation data were plotted as final tubulin concentration (C_t) versus $1/\tau^2$ and fit by linear regression. $1/\tau^2 = 4\,k_a k_d M^{-1} C_t + k_d^2$ (Thusius *et al*., 1975), where M is the molecular weight of the tubulin heterodimer, 100,000 Da.

here that exchange of liganded heterodimers in vinflunine-induced tubulin spirals is even more rapid than that in vinorelbine-induced spirals. Thus, in the presence of either vinorelbine or vinflunine, tubulin heterodimers are more readily exposed to alkylation than when vinblastine or vincristine is present. This differential exposure of sulfhydryls can occur even though the conformations of the drug-induced spirals are similar.

Analysis of the sedimentation velocity data in terms of overall binding affinity, K_1K_2, has shown that the order of vincristine > vinblastine > vinorelbine (Lobert *et al.*, 1996). For data fit with the ligand-mediated model, the difference $\Delta G_{vincristine} - \Delta G_{vinblastine}$, or $\Delta\Delta G°$, is 0.68 kcal/mol. Comparing the same model fits for vinblastine minus the data reported here for vinorelbine, we find that $\Delta G_{vinblastine} - \Delta G_{vinorelbine}$, $\Delta\Delta G°$, is 0.88 kcal/mol. The difference between vinorelbine and vinflunine, $\Delta G_{vinorelbine} - \Delta G_{vinflunine}$, amounts to a $\Delta\Delta G°$ value of 1.00 kcal/mol. Data fit with the combined model show the same trends, but the magnitudes of the differences are somewhat smaller. Thus, vinorelbine-induced tubulin self-association is favored relative to vinflunine as demonstrated by sedimentation velocity data and supported by the kinetic data.

When individual parameters are examined, we find that the binding affinity of vinorelbine, vinblastine, or vincristine for tubulin heterodimers, K_1, is identical within error for all three drugs, $1.6 \pm 0.3 \times 10^5\ M^{-1}$ at 25° (Lobert *et al.*, 1996). For the vinorelbine and vinflunine data reported here at 25°, the mean K_1 value is $9.6 \pm 2.7 \times 10^4\ M^{-1}$. Thus, there is no significant difference in the affinity of tubulin heterodimers for any of the vinca alkaloids studied. As found with vinorelbine, vinblastine, and vincristine, the major differences between vinorelbine and vinflunine are in the affinity of liganded heterodimers for polymers, K_2, and in the affinity of drug for polymers, K_3.

GDP enhances vincristine-, vinblastine-, and vinorelbine-induced tubulin self-assembly relative to GTP by 0.90 ± 0.17 kcal/mol (Lobert *et al.*, 1996). In the work described here, we find the same GDP enhancement of vinorelbine- and vinflunine-induced tubulin spiral formation, 0.84 ± 0.20 kcal/mol. The GDP enhancement occurs primarily in K_2 and K_3. It seems that GDP enhancement must be due to an intrinsic allosteric feature of the tubulin structure. The GDP enhancement of vinca alkaloid-induced tubulin self-association observed now with four vinca alkaloids, vincristine, vinblastine, vinorelbine, and vinflunine suggests that spirals may propagate into the microtubule core by a zipper-like or protofilament-peeling mechanism (Himes, 1991; Lobert *et al.*, 1995). These results indicate that a destabilizing effect on the GDP core of microtubules is a common mechanism in vinca alkaloid chemotherapeutics. Our kinetic results indicate that spirals or liganded heterodimers could associate with microtubule ends, suppressing dynamics. All four vinca alkaloids have the same energetic potential for propagation of spirals into the microtubule core and disrupting lateral interactions. Thus, a nucleotide-dependent allosteric effect is exhibited by all vinca alkaloids, such that drug binding induces the same cooperative depolymerization of mitotic spindles.

Implications for *in vivo* chemotherapeutic effects. Biosynthesis of vinca alkaloids involves a coupling reaction of the two precursors, catharanthine and vindoline. During this reaction, catharanthine undergoes a rearrangement to the cleavamine skeleton. This structure is not directly comparable to that of catharanthine. However, Prakash and Timasheff (1991) found that catharanthine will inhibit microtubule polymerization *in vitro* and induce tubulin self-association, although the magnitude of the effect is less than the "dimeric" vinblastine or vincristine. Borman and Kuehne (1989) showed that modification of vinblastine at the C4′ position alters the drug activity *in vitro* and *in vivo*. Vinorelbine is a vinblastine derivative modified at C4′ with an eight- instead of the nine-membered C′ ring of the natural compounds. It was synthesized in the late 1970s (Mangeney *et al.*, 1979) and shown to have a different spectrum of clinical activity from vincristine and vinblastine and an improved toxicity profile in cancer patients (Johnson *et al.*, 1996). Our biophysical studies demonstrate that vinorelbine binds to tubulin with much weaker overall affinity, K_1K_2, than vinblastine or vincristine, resulting in the formation of smaller spirals. The weaker binding is not in the drug binding to tubulin heterodimers but rather in the affinity of liganded heterodimers for spiral polymers. This results in the formation of smaller spirals. The results presented here demonstrate that vinflunine is a tubulin-binding drug, inducing smaller spirals than vinorelbine. These data suggest that like other vinca alkaloids, the antineoplastic effects of vinflunine are a direct result of its interaction with mitotic spindles, most likely in the form of small liganded spiral polymers. We want to stress that this a novel way of thinking about the mode of action of this class of antineoplastic agents.

We hypothesize that reduced neurotoxicity of vinorelbine compared with that of vincristine is due to two coupled phenomena. First, less vinorelbine binds, and therefore less tubulin is bound to these smaller spirals. Second, small spirals have a more rapid relaxation time and thus a potential for faster clearance from cells. It is well known that vinca alkaloid retention in cells and tissues correlates with drug potency (Houghton *et al.*, 1984, 1987; Gout *et al.*, 1984; Ferguson and Cass, 1985; Mullin *et al.*, 1985; Sirotnak *et al.*, 1986). It is very likely that drug-induced tubulin spiraling contributes to drug retention and cytotoxicity. Larger spirals should result in longer intracellular drug retention, as found with vincristine compared with vinblastine (Houghton *et al.*, 1987). We showed that for vinorelbine, vinblastine, and vincristine, drug spiraling correlates with clinical doses and toxicity (Lobert *et al.*, 1996). Most recently, vinflunine, a difluorinated derivative of vinorelbine, modified uniquely at the C20′ position with a reduction of the 3′,4′ double bond on the cleavamine moiety (Fahy *et al.*, 1997) has demonstrated preclinical antineoplastic activity. Definite *in vivo* antitumor activity has been demonstrated (Kruczynski *et al.*, 1998b) and *in vitro* mitotic arresting and tubulin interacting properties have been identified (Barret *et al.*, 1997). Specifically, the four vincas differentially interfere with the binding of tritiated vincas to tubulin as follows: vincristine > vinblastine > vinorelbine > vinflunine. Consistent with these findings, we have shown in the studies described here that vinflunine binds with several-fold lower overall affinity to tubulin than vinorelbine and, consequently, induces smaller spirals with a more rapid relaxation time. Thus, according to our hypothesis, we predict that vinflunine will have reduced toxicity compared with other vinca alkaloids.

There are conflicting reports comparing *in vitro* drug binding affinities and *in vivo* cytotoxicity. Plasma drug levels at steady state reach nanomolar concentrations. Furthermore, relative to extracellular levels, vinca alkaloids accumulate in

cells several-fold to ≥100-fold depending on the cell type (Gout *et al*., 1984; Jordan *et al*., 1991). Intracellular drug concentrations remain substoichiometric relative to the intracellular tubulin, which is estimated to be near 20 μM (Jordan *et al*., 1991). One study indicated that although vindesine binds to tubulin with lower affinity than vincristine, it has greater efficacy when B16 melanoma cells are exposed for 2 hr and transplanted into mice (Jordan *et al*., 1985). A later study demonstrated comparable cytotoxic effects in B16 melanoma cells for vincristine and vindesine after 43-hr exposure (Singer and Himes, 1992). In the same study, vinepidine was found to be less cytotoxic than vincristine, although its K_{app} value was larger. However, vinepidine uptake into cells was by far the lowest after 90-min exposure. Clearly, duration of exposure of cells to vincas is an important contributor to cytotoxicity. It should be noted that in cancer patients, the plasma terminal half-lives of these drugs are 1–3.5 days. Therefore, tissues are exposed to drugs over a period of several days. In fact, in animal studies, vinepidine plasma levels have not reached plateau even at 72 hr, and its cytotoxicity falls between vinblastine and vincristine (Mullin *et al*., 1985). We now have data showing that the overall affinity of vinepidine for tubulin falls between vincristine and vinblastine (Lobert and Correia, 1997). Our studies reported here suggest that the formation of larger spirals results in relatively longer retention in cells and tissues and greater potential for toxicity, as observed with vincristine and vinepidine. This does not exclude the importance of other parameters that contribute to pharmacokinetics (e.g., lipid solubility and drug uptake into tissues and cells). Additional factors that lead to prolonging the drug terminal half-life may also contribute to toxicity. We assert that all of these factors are important for a quantitative understanding of the time course for cellular and clinical toxicity.

Acknowledgments

We wish to thank Drs. Jacques Fahy and Jean-Marc Barret (Center de Recherche Pierre Fabre, Castres, France) for critical reading and helpful discussions during the preparation of this manuscript. We are grateful to the University of Mississippi Analytical Ultracentrifuge Facility and the Institut de Recherche Pierre Fabre for their support. Finally, we thank Pelahatchie Country Meat Packers for providing pig heads for tubulin purification. This is UMC AUF publication 0013.

References

Amos LA, Jubb JS, Henderson R, and Vigers G (1984) Arrangement of protofilaments in two forms of tubulin crystal induced by vinblastine. *J Mol Biol* **178:**711–729.

Barret J-M, Kruczynski A, Etievant C, Limouzy A, Rigaud S, Cabrol N, Gras S, Fahy J, Colpaert F, and Hill BT (1997) Characterization of the *in vitro* activity of F12158, a novel vinca alkaloid derivative with in vivo antitumor activity. *Proc Am Assoc Cancer Res* **38:**226.

Borman LS and Kuehne ME (1989) Specific alterations in the biological activities of c-20′-modified vinblastine congeners. *Biochem Pharmacol* **38:**715–724.

Chabner BA, Allegra CJ, Curt GA, and Calabresi P (1996) Antineoplastic agents, in *Goodman and Gilman's The Pharmacological Basis of Therapeutics* (Hardman JG, Limbird LM, Molinoff PB, Ruddon RW, and Gilman AG, eds) pp 1233–1287, McGraw- Hill, New York.

Correia JJ, Baty LT, and Williams RC Jr (1987) Mg^{2+} dependence of guanine nucleotide binding to tubulin. *J Biol Chem* **262:**17278–17284.

Detrich HW and Williams RC Jr (1978) Reversible dissociation of the $\alpha\beta$ dimer of tubulin from bovine brain. *Biochemistry* **17:**3900–3907.

Fahy J, Duflos A, Jacquesy JC, Jouannetaud MP, Meheust C, Kruczynski A, Etievant C, Barret JM, Colpaert F, and Hill BT (1997) *Vinca* alkaloids in superacidic media: a method for creating a new family of antitumor derivatives. *J Am Chem Soc* **119:**8576–8577.

Ferguson PJ and Cass CE (1985) Differential cellular retention of vincristine and vinblastine by cultured human promyelocytic leukemia HL-60/C1 cells: the basis of differential toxicity. *Cancer Res* **45:**5480–5488.

Fujiwara K and Tilney LG (1975) Structural analysis of the microtubule and its polymorphic forms. *Ann N Y Acad Sci* **253:**27–50.

Gout PW, Noble RL, Bruchovsky N, and Beer CT (1984) Vincristine and vinblastine—growth-inhibitory effects correlate with their retention by cultured Nb2 node lymphoma cells. *Eur J Cancer* **34:**245–248.

Himes RH (1991) Interactions of the Catharanthus (vinca) alkaloids with tubulin and microtubules. *Pharmacol Ther* **51:**257–267.

Houghton JA, Williams LG, Dodge RK, George SL, Hazelton BJ, and Houghton PJ (1987) Relationship between binding affinity, retention and sensitivity of hymen rhabdomyosarcoma xenografts to vinca alkaloids. *Biochem Pharmacol* **36:**81–88.

Houghton JA, Williams LG, Torrance PM, and Houghton PJ (1984) Determinants of intrinsic sensitivity to vinca alkaloids in xenografts of pediatric rhabdomyosarcomas. *Cancer Res* **44:**582–590.

Johnson SA, Harper P, Hortobagyi GN, and Pouillart P (1996) Vinorelbine: an overview. *Cancer Treat Rev* **22:**127–142.

Jordan MA, Himes RH, and Wilson L (1985) Comparison of the effects of vinblastine, vincristine, vindesine, and vinepidine on microtubule dynamics and cell proliferation in vitro. *Cancer Res* **45:**2741–2747.

Jordan MA, Thrower D, and Wilson L (1991) Mechanism of inhibition of cell proliferation by vinca alkaloids. *Cancer Res* **51:**2212–2222.

Jordan MA and Wilson L (1990) Kinetic analysis of tubulin exchange at microtubule ends at low vinblastine concentrations. *Biochemistry* **29:**2730–2739.

Kruczynski A, Barret JM, Etievant C, Colpaert F, Fahy J, and Hill BT (1998a) Antimitotic and tubulin interacting properties of a novel fluorinated *Vinca* alkaloid, vinflunine. *Biochem Pharmacol* **55:**635–648.

Kruczynski A, Colpaert F, Tarayre JP, Mouillard P, Fahy J, and Hill BT (1998b) Preclinical *in vivo* antitumour activity of vinflunine, a novel fluorinated *Vinca* alkaloid. *Cancer Chemother Pharmacol*, in press.

Liu S and Stafford WF III (1995) An optical thermometer for direct measurement of cell temperature in the Beckman Instruments XL-A analytical ultracentrifuge. *Ann Biochem* **224:**199–202.

Lobert S, Boyd CA, and Correia JJ (1997) Divalent cation and ionic strength effects on vinca alkaloid-induced tubulin self-association. *Biophys J* **72:**416–427.

Lobert S and Correia JJ (1992) Antimitotics in cancer chemotherapy *Cancer Nursing* **15:**22–33.

Lobert S and Correia JJ (1997) Thermodynamics of vinca alkaloid-induced tubulin self- association. *Prot Sci* **6**(Suppl 2)**:** 81.

Lobert S, Frankfurter A, and Correia JJ (1995) Binding of vinblastine to phosphocellulose-purified and $\alpha\beta$-class III tubulin: the role of nucleotides and β-tubulin isotypes. *Biochemistry* **34:**8050–8060.

Lobert S, Vulevic B, and Correia JJ (1996) Interaction of vinca alkaloids with tubulin: a comparison of vinblastine, vincristine and vinorelbine. *Biochemistry* **35:**6806–6814.

Mangeney P, Andriamialisoa RZ, Langlois N, Langlois Y, and Potier P (1979) A new class of antitumor compounds: 5′-nor and 5′,6′-seco derivatives of vinblastine-type alkaloids. *J Org Chem* **44:**3765–3768.

Mullin K, Houghton PJ, Houghton JA, and Horowitz ME (1985) Studies with 4′-deoxyepivincristine (vinepidine), a semisynthetic vinca alkaloid. *Biochem Pharmacol*. **34:**1975–1979.

Na GC and Timasheff SN (1980) Thermodynamic linkage between tubulin self-association and the binding of vinblastine. *Biochemistry* **19:**1347–1354.

Na GC and Timasheff SN (1985) Velocity sedimentation study of ligand-induced protein self-association. *Methods Enzymol* **117:**459–495.

Na GC and Timasheff SN (1986a) Interaction of vinblastine with calf brain tubulin: multiple equilibria. *Biochemistry* **25:**6214–6222.

Na GC and Timasheff SN (1986b) Interaction of vinblastine with calf brain tubulin: effects of magnesium ions. *Biochemistry* **25:**6222–6228.

Nogales E, Medrano FJ, Diakun GP, Mant GR, Towns-Andrews E and Bordas J (1995) The effect of temperature on the structure of vinblastine-induced polymers of purified tubulin: detection of a reversible conformational change. *J Mol Biol* **254:**416–430.

Prakash V and Timasheff SN (1991) Mechanism of interaction of vinca alkaloids with tubulin: catharanthine and vindoline *Biochemistry* **30:**873–880.

Singer WD and Himes RH (1992) Cellular uptake and tubulin binding properties of four vinca alkaloids. *Biochemical Pharmacol* **43:**545–551.

Sirotnak FM, Yang C-H, Mines LS, Oribe E, and Biedler JLJ (1986) Markedly altered membrane transport and intracellular binding of vincristine in multidrug-resistant Chinese hamster cells selected for resistance to vinca alkaloids. *Cell Physiol* **126:**266–274.

Thusius D, Dessen P, and Jallon JM (1975) Mechanism of bovine liver glutamate dehydrogenase self-association: I. Kinetic evidence for a random association of polymer chains. *J Mol Biol* **92:**413–432.

Toso RJ, Jordan MA, Farrell KW, Matsumoto B, and Wilson L (1993) Kinetic stabilization of microtubule dynamic instability in vitro by vinblastine. *Biochemistry* **32:**1285–1293.

Williams RC Jr and Lee JC (1982) Preparation of tubulin from brain. *Methods Enzymol* 376–408.

Wyman J (1964) Linked functions and reciprocal effects in hemoglobin: a second look. *Adv Protein Chem* **19:**223–386.

Send reprint requests to: Dr. Sharon Lobert, University of Mississippi Medical Center, School of Nursing and Department of Biochemistry, 2500 N. State St., Jackson, MS 39216. E-mail: slobert@fiona.umsmed.edu.